UNIVERSITY OF CALIFORNIA,
IRVINE

A Complementary Microfluidic Device for Droplet-Based Single Cell Studies with an AFM System

THESIS

submitted in partial satisfaction of the requirements
for the degree of

MASTER OF SCIENCE

in Engineering with a concentration in Materials
and Manufacturing Technology

by

Ryan Lee Sanford

Thesis Committee:
Professor Abraham Lee, Chair
Professor Michelle Khine
Professor Chin Lee

2014

DEDICATION

To

my parents, family, and friends who have given

me unconditional support, motivation, and love to succeed

and excel. Without them, this thesis and my advanced

degree would not have been possible.

Imagination is more important than knowledge. For while knowledge
defines all we currently know and understand, imagination
points to all we might yet discover and create.

–Albert Einstein

What most of us present to the world isn't necessarily our true self:
It's a combination of years of bad habits and fear-based behavior.
Our real self lies buried underneath all the insecurities and inhibitions.
So rather than just being yourself, focus on discovering and
permanently bringing to the surface your best self.

–Neil Strauss

TABLE OF CONTENTS

LIST OF FIGURES

LIST OF TABLES

ACKNOWLEDGMENTS

I would like to express the deepest appreciation to my committee chair, Professor Abraham Lee, who first inspired my interest and fascination with microfluidics. His nurturing demeanor and excitement for learning encouraged open discussions and a facile exchange of ideas. His vision for open-access microfluidics and the possibilities it could create inspired the focus of this thesis. Without his continual guidance and support this thesis would not have been possible.

I would like to thank my lab members in BioMiNT who shared countless conversations with me which inspired many ideas and techniques in this research. They also taught me many of the operating procedures and methods which were critical to this research.

In addition, a thank you to Roger Yinglei Tao for discussing and demonstrating the AFM system developed by Dr. Kumar Wickramasinghe with me.

I thank the Weitz group at Harvard for publishing their work on their 'DropSpot' device. The principles demonstrated in their work provided a crucial basis in developing a device in this research. Financial support was provided by the University of California, Irvine.

ABSTRACT OF THE THESIS

A Complementary Microfluidic Device for
Droplet-Based Single Cell Studies with an AFM System

By

Ryan Lee Sanford

Master of Science in Engineering with a concentration in
Materials and Manufacturing Technology

University of California, Irvine, 2014

Professor Abraham Lee, Chair

The atomic force microscope (AFM) has become an extremely powerful tool for biological and cell studies. Modified AFM probes have been designed to inject biomolecules (DNA, proteins, etc.) into living cells or extract target biomolecules expressed inside the cells. However, the need for statistically significant sample sizes makes data collection an extremely lengthy process. A complementary microfluidic device can decrease data collection time by flowing cells passed the probe tip and immobilizing them while the probe investigates or manipulates the cell. Microfluidic devices generally do not permit physical access to channels and the ability to add or remove material is restricted to designated inlets and outlets, endpoints in microfluidic devices. True open-access microfluidics suffers from low pressure and flow rate limitations and an inability to integrate multiple modules. This research demonstrates a microfluidic device which can encapsulate cells within droplets, immobilize droplets, and release droplets to collect and analyze. Sealing the device with a thin film of PDMS provides the liberty for a probe to

inject, extract, or inspect material from any portion of the channels while providing a barrier to confine the fluid to within the channels during device operation.

CHAPTER 1: INTRODUCTION

Microfluidic Droplet-Based Single Cell Analysis

Single cell analysis has become an important diagnostic tool to gather statistical information about heterogeneities within cell populations. The distributions of these heterogeneities in cell populations have been found to differ substantially from Gaussian distributions, making assumptions of cell populations based on normal distribution inaccurate. To accurately describe these heterogeneities requires the analysis of single cells in large enough numbers to correctly represent the population. One preeminent high-throughput single cell analysis technique, called laser flow cytometry, uses laser light to analyze the presence of fluorescent molecules and the light-scattering properties of single cells as they move in single file past a detector. Cells can be analyzed at a rate as high as tens of thousands of cells per second. This technique is ideal for single time-point screening or population analysis of protein expression. However, due to a lack of robust compartmentalization, this technique is incompatible to track specific cells over time, analyze secreted products, and analyze behavior of isolated cells.[1]

Droplet-based microfluidics is one approach to compartmentalize single cells within its own aqueous vesicle. By encapsulating single cells within picoliter-sized droplets, quantitative studies of large populations of single cells can be conducted. Droplets provide well-defined environments for individual cells, isolating single cells and reagents in monodisperse picoliter vessels. The droplets entrap secretion products of the individual cells and prevent mixing with other cells. Additionally, the uptake of trace chemicals can be probed by their depletion within the confined droplet.[2] Furthermore, the low volumes of

droplets make large studies economically viable. The ability to generate and manipulate thousands of droplets per second allows the analysis to accurately describe a heterogeneous cell population. These qualities make droplet-based single cell analysis an attractive method to overcome the limitations of current single cell analysis techniques.

Encapsulating cells within droplets is typically a random process accomplished by diluting the suspension of cells, resulting in a population of droplets with a Poisson distributed cell occupancy. Poisson statistics are given as:

$$P(\lambda; k) = \lambda^k \exp(-\lambda) / k! \qquad (1)$$

where k is the number of cells in the droplet and λ is the average number of cells per droplet, which can be adjusted by controlling the density of cells suspended.[3] Because very low loading densities are required to minimize the number of droplets that contain multiple cells, the majority of droplets are empty. In order to minimize this inefficiency, various methods have been developed, such as hydrodynamic sorting, inertial focusing, and elaborate detection systems.[2]

Surfactants are not essential for the generation of droplets, but droplets not stabilized by surfactants will coalesce upon contact after formation. Two important characteristics of an oil and aqueous-phase surfactant system are described by interfacial tension and the critical micellar concentration (CMC), the surfactant concentration at which the interfacial tension reaches a minimum. A general requirement for droplet stabilization is possessing an interfacial tension value between the two phases of less than 20 mN/m.[4]

For biochemical applications, the oil phase, aqueous phase, and surfactant must be biocompatible. The oil–water interface must appear as inert as possible to the droplet content. With miniaturization, interfacial effects become predominant compared to bulk.

The surface effects must be minimized so the oil–water interface appears as inert as possible to the droplet content. Miniaturization can also limit the amount of nutrients available to the biological contents. Fluorocarbon oils are appealing choices and have advantages over hydrocarbon oils. Fluorocarbon oils offer superior oxygen transport properties to support cell respiration and are insoluble to most organic compounds and aqueous solvents.[5]

The Atomic Force Microscope for Biological Studies

The atomic force microscope (AFM) has become an extremely powerful tool for biological studies due to its subnanometric resolution and ability to manipulate biomolecules. The AFM is capable of imaging biological samples such as DNA, proteins, and living cells at the molecular level under near-physiological conditions and can characterize localized mechanical properties of these cells, such as hardness and elasticity. Modified AFM probes have been designed to inject biomolecules (DNA, proteins, etc.) into living cells and extract target biomolecules expressed inside the cells.[6] The ability to inject materials such as proteins, DNA, and drugs into individual cells is applicable across a wide array of areas, especially therapeutic development. Specific injection or extraction enables research at the single-cell level due to its ability to target specific cells.[7]

Research published by the Wickramasinghe group at UC Irvine demonstrated selective mRNA extraction and quantification through the use of a modified AFM probe, shown in Figure 1.[8] Dubbed a dielectric nanotweezer (DENT), they describe the DENT as a tapered, nanoscale coaxial cable integrated into an AFM probe. The application of an AC electric field between the inner and outer electrodes of the DENT creates a large electric

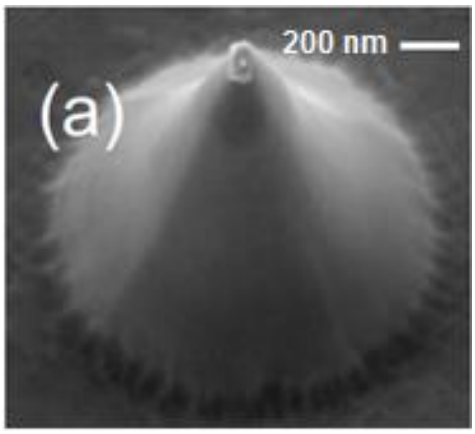

Figure 1: Scanning electron microscope image of structurally modified AFM tip (DENT).[8]

field gradient at the probe tip, resulting in a dielectrophoretic attractive force on mRNA molecules. The group was able to achieve selective mRNA extraction by combining the positive dielectrophoretic force which attracts mRNA molecules toward the probe tip with chemical derivatization of the probe surface using gene specific oligonucleotide primers tailored to hybridize the specific target mRNA. The mRNA expression experiments were performed by inserting the modified AFM probes into the nucleus of the cell and applying a 120 KHz, 5 V peak-to-peak AC voltage signal across the inner and outer electrodes of the DENT for 60 seconds. Then the probe tip was extracted with the captured mRNA, mRNA was released in DI water and then finally analyzed using gel electrophoresis or quantitative polymerase chain reaction (qPCR).[8,9]

Modified AFM probes have also been designed to introduce biomolecules and active reagents into living cells. One method, known as Dip-Pen Nanolithography, simply dips the AFM probe tip into a solution and then deposits it into a cell by poking through its membrane.[10] The integration of nanofluidic channels onto the AFM cantilever allows continuous flow of material to the tip. These designs penetrate the cell membrane with a

sharp tip and then pump solution into the cell.[6,7,10,11,12] Figure 2 shows a schematic and scanning electron microscopy image of one type of design, the FluidFM.[12] Solution can be injected through the tip by applying an external pressure or driven elecrokinetically.[6]

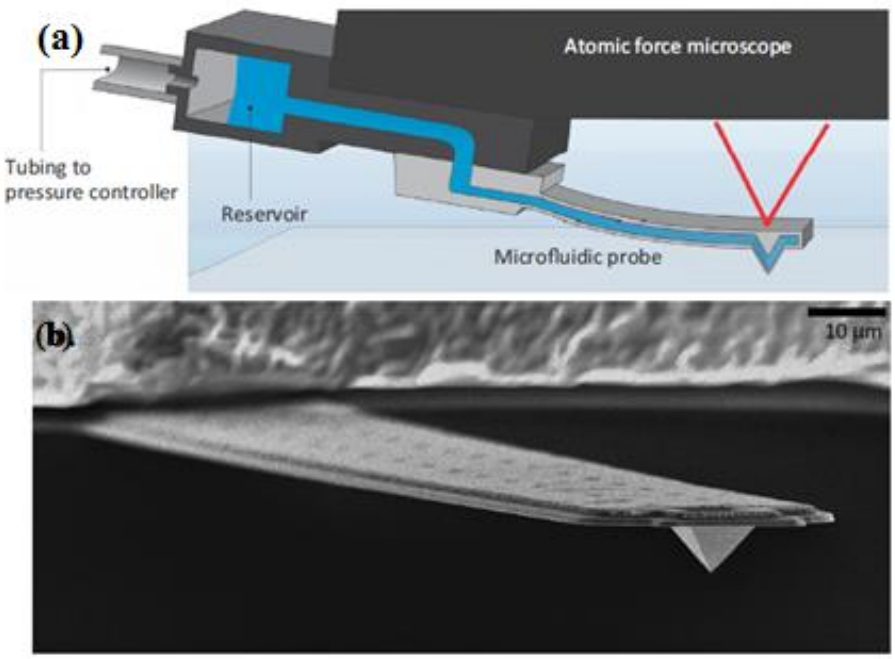

Figure 2: Microchanneled AFM cantilever for fluidic force microscopy (FluidFM) (a) Schematic of a FluidFM system, combining an atomic force microscope with a microfluidic probe on top of an inverted optical microscope. (b) Scanning electron microscopy image of AFM cantilever. [12]

Currently, the AFM probe locates cells on a glass slide by using a cantilever to establish contact with the cell.[7,8,9,10,12,13] A complementary microfluidic device can decrease data collection time by flowing cells passed the probe tip, immobilizing them while the probe investigates or manipulates the cell and then releasing them to accept the next. Secondly, parallel operation within a single system can increase its productivity. To perform parallel AFM experiments within a microfluidic chip, an array of probe tips must be integrated on a single chip due to space limitations. One group from Switzerland

fabricated an array of AFM probes capable of performing parallel force microscopy on living cells and demonstrated its viability.[13]

Accessing Microfluidic Channels

Most microfluidic devices are closed systems with no way of accessing the contents within the channels until it flows through to an outlet. Many techniques have been studied and utilized for "open-access" microfluidics, microfluidic devices with open channels. Many of these methods take advantage of hydrophobic and hydrophilic surfaces to trace out paths and channels. Various driving forces include flow-controlled pumping, chemotaxis, and paper-based capillary forces to pump liquid through the device.[14,15,16] One device has even demonstrated single and double emulsion generation in an open-access environment.[17] However, these true open-access microfluidic devices cannot integrate more than a few simple microfluidic modules and can only employ low, limited flow rates and pressures. In order to access microfluidic channels without incurring the limitations of true open-access microfluidics, devices can be sealed with a thin film membrane.

Sealing a microfluidic device with a thin film membrane provides a unique solution to allow physical access to microfluidic channels while overcoming some limitations of true open-access microfluidics. The thin membrane confines the fluid within the channels at much higher pressures and flow rates than in a true open-access device. To access contents within microfluidic channels, access points can be created by puncturing the film with a sharp tool or laser. The size and shape of the access points can be tailored, and can easily be smaller than the width of the channel.

The size of the access points affect the maximum allowable pressure within the device before leaking occurs. The amount of pressure the fluid can support before leaking through the access point can be described by the Young-Laplace Equation:

$$\Delta p = \gamma \left(\frac{1}{R_1} + \frac{1}{R_2} \right) \qquad (2)$$

where γ is the interfacial tension between the liquid and air, and R_1 and R_2 are the principal radii of curvature.[18] Increasing the interfacial energy and decreasing the radii of the access point will increase the maximum pressure allowed before leaking occurs.

The elasticity of the thin film membrane also affects the behavior of the access points. Membranes which are more elastic can stretch elastically around the girth of the needle. As the needle is removed, elastic relaxation of the molecules occurs, effectively making the puncture hole to be smaller than the diameter of the needle. This effect should be negligible when fabricating access holes thermally with a laser. Similarly, the elasticity of the film can also cause access points to enlarge elastically, even plastically, if sufficient pressure is applied. This can increase the size of the access point and cause fluid leakage at lower pressure values than calculated with a static model.

Membrane deflection due to pressure is another consequence to consider when choosing the elastic modulus of the membrane. Decreasing the elasticity of the membrane increases the compliance of the membrane. Compliance exists because neither real fluids nor the confining chambers or channels are completely rigid. Compliance of the film causes it to acts like a spring by absorbing energy as it deflects elastically. When the pressure is reduced or removed, the potential energy of the membrane is released as it relaxes and causes flow to continue after the external pressure is removed.

Thin plate or small deflection theory is appropriate for deflections less than 1/5 of the membrane thickness. Large deflection or membrane theory can estimate deflections up to three times the membrane thickness more accurately. Thin plate or small deflection theory is dominated by the resistance of the membrane to bending. The deflection, D, of a clamped circular plate under a uniform applied pressure, P, is given by:

$$D(r) = \frac{Pa^4}{64F}\left[1 - \left(\frac{r}{a}\right)^2\right]^2 \qquad (3)$$

where r, is the radial coordinate, a is the membrane radius, and F is the flexural rigidity, which is a measurement of stiffness, and is given by:

$$F = \frac{Et^3}{12(1-\nu^2)} \qquad (4)$$

where E, t, and ν are the Young's modulus, plate thickness, and Poisson's ratio, respectively. In contrast, deflection in membrane theory is dominated by stresses in the plate:

$$D(r) = \frac{Pa^4}{4\sigma_i h}\left[1 - \left(\frac{r}{a}\right)^2\right]^2 \qquad (5)$$

where σ_i is the intrinsic stress of the plate. The two approaches are nearly the same for small deflections and diverge for larger deflections, with thin plate theory overestimating the actual deflection.[19]

Probe tips can also induce a local negative deflection of the membrane during probing. Membranes with a lower elastic modulus will undergo a greater deflection before puncture occurs. If the membrane is very elastic or if the tip is not very sharp, the deflection of the membrane can be great enough to disrupt the contents of the microfluidic channel and push them away from the access point. This issue can be circumvented by pre-puncturing the film at the access point locations before running the experiment.

The strength of the thin film membrane ultimately limits the maximum pressure which can be employed in the device. The highest pressure experienced by the thin film will be experienced at the inlets, and rupture may occur if a maximum pressure is exceeded.

Device Design Concept

This research aimed to decrease data collection time of single cell studies conducted by AFM probes by developing a complementary microfluidic device which can flow cells to probe tip, immobilize them while the probe investigates or manipulates the cell, and then release them to accept the next wave of cells. It also aims to incorporate the advantages of droplet single cell studies. The design objectives of the device are:

1. The device encapsulates live cells in aqueous droplets.
2. Droplets can flow to the AFM probe on demand.
3. The device immobilizes droplets so they may be probed.
4. The AFM probe is able to access cells within the immobilized droplets.
5. Droplets can be released for collection and analysis.

A schematic of the device is shown in Figure 3.

In order to generate droplets and effectively trap and release droplets on demand, this research borrows principles utilized by the 'DropSpot' device. Pioneered by the Weitz group at Harvard, DropSpot is a microfluidic device that uses an array of chambers to immobilize aqueous droplets suspended oil. This unique solution enables time-lapse studies of large populations of cells and simple recovery of the droplets. The design flows droplets through an array of round chambers connected by narrow constrictions. When

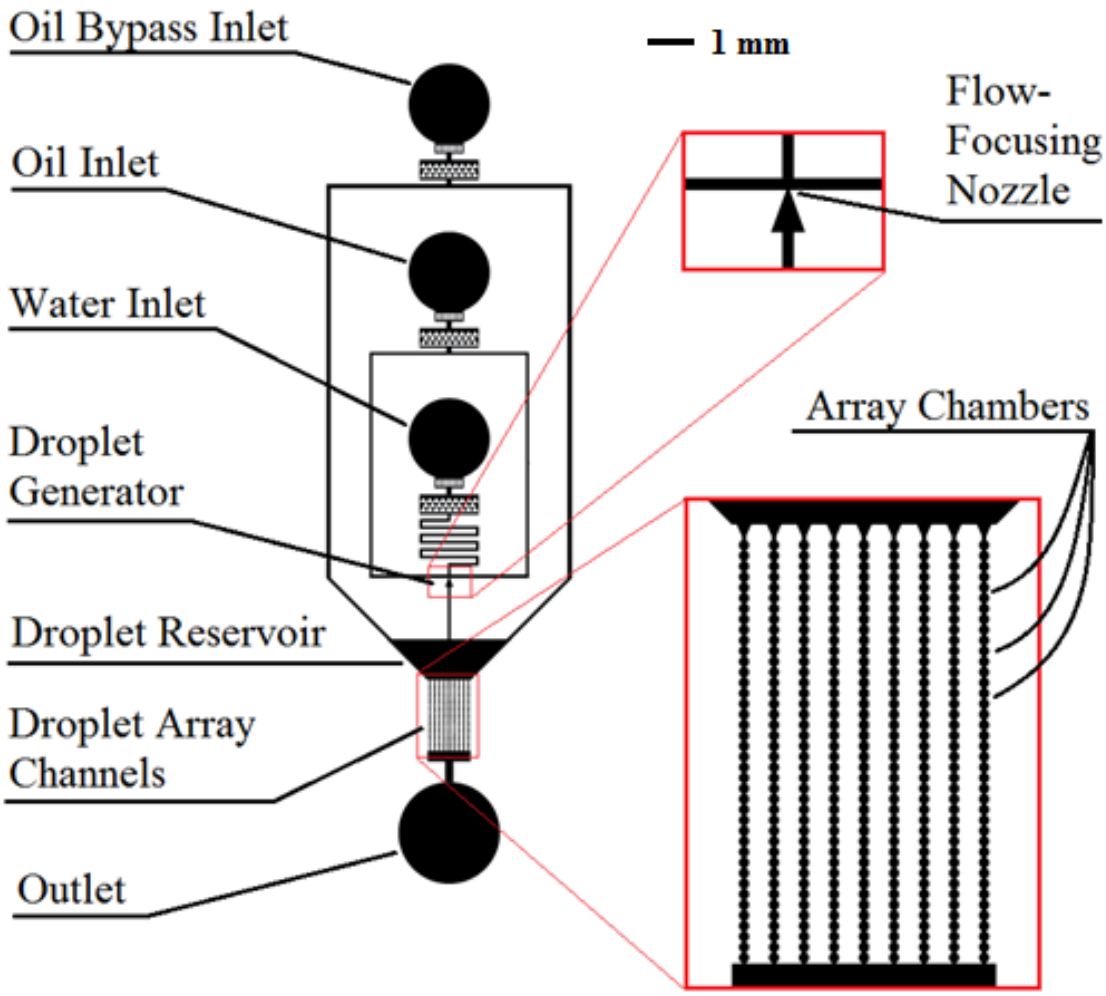

Figure 3: Schematic drawing of the microfluidic chip. Black areas correspond to microfluidic channels.

sufficient pressure is applied, droplets can squeeze through the constrictions. Once pressure is removed, the surface tension drives droplets to their lowest energy shape and traps droplets within the chamber.[20]

Next, the AFM probe must be able to access the droplets within the microfluidic channel. Because AFM probes are incredibly short (<60 μm), the device was sealed with a thin film membrane of polydimethylsiloxane (PDMS). Two methods were investigated to fabricate the thin film and seal the device.

CHAPTER 2: DEVICE FABRICATION AND EXPERIMENTAL SET-UP

Device Fabrication

Hard molds were fabricated in the cleanroom using lithographic techniques according to the operating procedures provided by MicroChem.[21] MicroChem negative photoresist SU-8 2025 (η = 4500 cSt, ρ= 1.219 g/mL) was spin coated onto a cleaned and dehydrated wafer at 3500 rpm, and then soft baked at 65°C for 1 minute and at 95°C for 5 minutes. The masks were designed in AutoCAD and were printed by CAD Art Services on a transparency at 20,000 dpi resolution. The mask pattern was transferred to the wafer through UV lithography with an AB&M UV Flood Exposure System Deep UV (220-280nm). A post-exposure bake was then carried out at 65°C for 1 minute and then 95°C for 5 minutes. After resist development, a hard bake was done at 150°C for 10 minutes. Lastly, the wafers were surface treated by spinning a Teflon solution onto the wafer at 1500 rpm, followed by a bake at 120°C for 2 minutes. The Teflon solution was made by mixing 3M FC-43 Fluorinert with DuPont Amorphous Fluoropolymer Solution in a 5:1 ratio by volume.

The microfluidic chips were fabricated from the hard mold by soft lithography with Sylgard 184 Polydimethylsiloxane (PDMS). The PDMS base and curing agents were mixed in a 5:1 ratio by weight. This mixture was degassed in vacuum, poured on top of the silicon wafer molds, and cured at 65°C overnight. The cured PDMS was then cut and peeled from the silicon wafer. Inlet and outlet holes were punched into the PDMS chips with a biopsy punch. Nitrogen gas and adhesive tape were used to remove any debris from the surface of the chips.

Thin Film Fabrication and Device Sealing

In order to allow the AFM probe to access the droplets within the microfluidic device, a thin film membrane was used to seal the device. Two methods were explored to fabricate PDMS thin films and seal the device: a Solvent Release Method and a Peel Method. Schematics and photos comparing the two methods are shown in Figure 4.

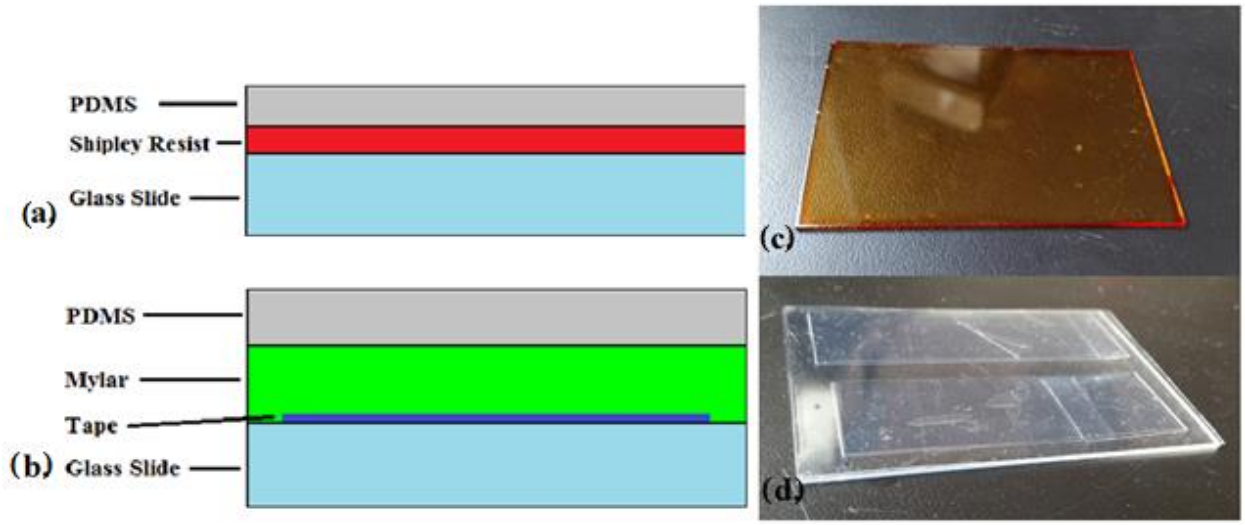

Figure 4: Comparison of slides fabricated for the Solvent Release Method and Peel Method. (a-b) Schematics illustrating the composition and order of layers on slide for each method (not drawn to scale). Photos of cured slides ready to be bonded to microfluidic chip via (c) Solvent Release Method and (d) Peel Method.

Solvent Release Method

In the Solvent Release Method, glass Corning Micro Slides (75 x 50 mm) were cleaned with acetone, methanol, and isopropyl alcohol, and dehydrated for 20 minutes in an oven at 120°C. Then, Shipley 1827 photoresist was spread across the glass and spun at 2500 rpm. This created a release layer between the PDMS thin film and the glass slide. The coated slides were soft-baked in an oven at 120°C for 5 minutes to eliminate its tackiness.

Then, degassed PDMS was spin coated onto the slides at 6000 rpm to yield an approximate membrane thickness of 10 microns. Figure 5 shows resulting thicknesses of PDMS films from various spin speeds.[22] The glass slides were then cured at 65°C overnight. Next, the slides and prepared PDMS chips were bonded together by treating the surfaces with oxygen plasma for two minutes and contact-bonded together, creating an irreversible covalent bond between the device and the thin film of PDMS. The sealed devices were then put in an oven at 120°C for at least two hours to increase the bond strength and restore the hydrophobicity of the PDMS.

Once sealed, the devices were placed in a shallow acetone bath to dissolve the Shipley photoresist and release the glass slide from the device, leaving a thin film of PDMS to seal the microfluidic chip. A squirt bottle was employed to flow fresh acetone between the glass slide and the device. Care was taken so that the solvent does not enter into the

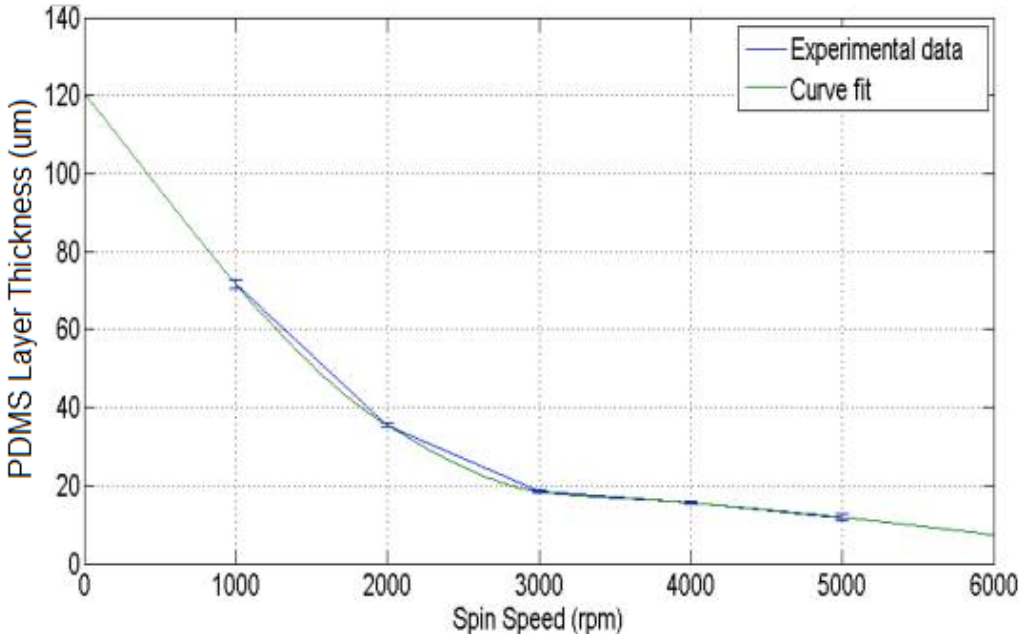

Figure 5: Plot of PDMS layer thickness (µm) versus spinner spin speeds (RPM) of 30 seconds. PDMS used has a 5:1 ratio of base: curing agent.[22]

device through the inlets or outlets. If solvent entered the device, the resist dissolved in the acetone hardened within the channels as the acetone evaporated, creating blockages which often rendered the device useless. Once a device has been completely released from the glass slide, it was rinsed with isopropyl alcohol. Drying with compressed air often broke the thin film membrane at the inlets and outlets, and was consequently not performed. Due to the porous nature of PDMS, swelling occurred through the absorption of the acetone. To remove any swelling incurred during the release stage, devices were placed in an oven at 65°C for an hour.

Peel Method

The Peel Method of fabricating PDMS thin films did not require a solvent bath. In this method, a film of Mylar was first cleaned with isopropyl alcohol and then taped to a glass slide with double-sided tape. The glass slide provided a rigid, flat surface to shape the PDMS thin film, and the Mylar provided a surface to which PDMS didn't stick to. Like the previous method, PDMS was spun on at 6000 rpm and then the slides were cured overnight at 65°C. The slides were bonded to the devices by treating the surfaces with oxygen plasma for two minutes, contact bonded, and then placed in an oven at 65°C for two hours. This lower temperature was necessary to prevent melting of the tape's adhesive and warping of the Mylar film. To release the PDMS thin film, the PDMS film was cut with a scalpel, tracing the outline of the device. Only the PDMS thin film was cut, not the Mylar. The tape was then cut to release the Mylar from the glass slide, and then the Mylar was carefully peeled from the device, leaving the PDMS chip sealed with a thin PDMS membrane. A device fabricated with the Peel Method is shown in Figure 6.

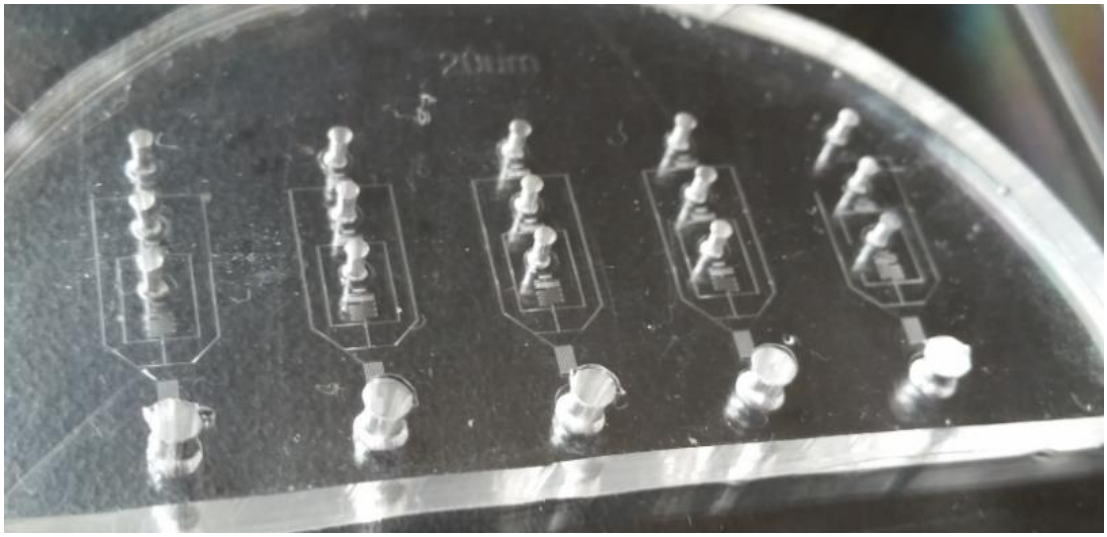

Figure 6: Photo of finished device fabricated via Peel Method. Contains 5 individual devices.

Experimental Set-up and Procedures

A surfactant-enriched mineral oil was made by mixing Sigma Span 80 with Sigma-Aldrich light mineral oil at a concentration of 0.03% (w/v), corresponding to its CMC. To facilitate optimum device performance, the device was first primed with the surfactant-enriched mineral oil by adding the oil to the outlet reservoir and allowing it to wick through the device via capillary force to each of the three outlets. Once oil has completely wicked through to the two oil inlets, they were filled with additional mineral oil using a syringe and needle. Deionized water was similarly added to the water inlet. After the tubing was primed, it was inserted into the device.

All experiments were conducted in a pressure-controlled regime using pressure pumps. Droplet generation was carried out by pressurizing the oil and water inlets. After the oil pressure was set, the water pressure was adjusted to achieve the correct droplet diameter. Typical pressures employed for droplet generation were 2 psi and 1.45 psi applied to the oil and water inlets, respectively. During this step, droplets flowed into the

reservoir and through the array channels. This step continued until the incorrectly sized droplets and any air bubbles were flushed through to the outlet, and only correctly sized droplets remained in the reservoir and array channels.

Once droplet generation was completed, the droplets in the array were probed using a MicroXact 500 series mechanical micropositioner and a GGB Industries Picoprobe T-4-22 tungsten probe tip. This step was designed to simulate cell probing with an AFM tip. The micropositioner was tilted at a 20° angle so that the point of the tip could be seen through the inverted microscope. The probe penetrated the thin film near the center of each chamber, into the trapped droplet, and was then retracted. Once all the droplets had been probed in the first row of array chambers, pressure was applied to the inlets and slowly increased until droplets began releasing. Pressure was applied to the oil bypass channel first, and the pressure applied to the oil and water inlets was adjusted to prevent droplets from flowing from the reservoir back to the inlets. Removing the tubing from the device caused a sudden pressure drop which greatly perturbed the droplets in the reservoir and array channel, and so tubing was not inserted or removed from the device during device operation. A total pressure of 1.5 psi was applied to the inlets when droplets began releasing, with the partial pressures applied to each inlet given as: 0.6 psi to the oil bypass channel, 0.45 psi to the water inlet, and 0.45 psi to the oil inlet. Then, probing was done again to the next wave of droplets arriving to the first row of array chambers, subsequently released, and repeated. At the end of the experiment, droplets were flushed through to the outlet by applying a pressure of 2 psi to the bypass oil inlet and 1.3 psi to the water and oil inlets.

CHAPTER 3: RESULTS AND DISCUSSION

Device Design Parameters

Key design parameters were studied to optimize the design objectives of the device. The objectives of successful device operation include encapsulating cells within droplets with a high viability, trapping droplets effectively so they don't migrate into another chamber during probing, and disallowing droplets from leaking out of the device through the access holes in the thin film created by the probe tip.

The target droplet diameter, flow-focusing nozzle width, and constriction width between array chambers were chosen to prevent lethal shearing forces on cells and support healthy cell growth. The droplet diameter was minimized to increase the effectiveness of AFM probing. First, the AFM must locate the cell within the droplet, and a larger droplet volume will increase the time needed to locate the cell. Second, once the AFM pokes through the thin film, it must move laterally to locate the cell. This lateral motion of the AFM tip may cause the access hole to stretch and enlarge somewhat, causing fluid leakage at lower pressures. The constriction widths were minimized to increase the effectiveness of droplet trapping. The array chamber diameter was chosen to be the same as the target droplet diameter to effectively immobilize the droplet. It was also observed that larger flow-focusing nozzle widths required more oil to shear the water and create droplets of a specific size than smaller nozzles. The nozzle width was then minimized to increase the water droplet to oil ratio so a higher density of water droplets can be collected in the reservoir and array.

The height of the channel was designed to be shorter than the diameter of the target droplet for two practical reasons. First, shorter channel depth increases the accessibility of the AFM probe to reach cells at the bottom of droplets and gives more flexibility to increase thin film thickness if more mechanical strength is needed. Second, if the channel height were the same as the droplet diameter, space would be present around the corners, as shown in Figure 7a. This gap would allow oil to flow around the droplets, and consequently result in unreliable droplet release which requires a higher pressure. A smaller channel height can deform droplets so they create a "plug" to prevent oil from flowing around it, like in Figure 7b.

After these considerations were made, the device parameters were chosen as: target droplet diameter = 40 μm, flow-focusing width = 20 μm, constriction width = 20 μm, and channel height = 25 μm. The device also contains 40 array chambers within each array channel, and 9 array channels.

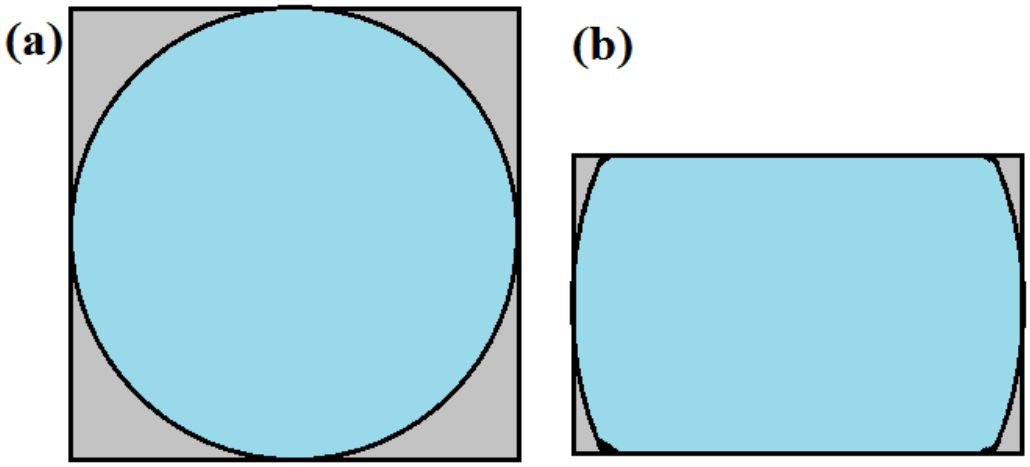

Figure 7: 2D illustration of a 40 μm droplet in (a) a square cross-section channel (40 x 40 μm) and in (b) a short, rectangular channel (40 x 25 μm). Illustrates the shrinking of the gaps around the droplet as droplet creates a "plug" when compressed.

Droplet Trapping and Releasing in Array

Theoretical Calculations

In order for droplets to move to the next array chamber, they must deform to squeeze through the constrictions. Due to the existence of a non-zero surface tension, a pressure drop is present across curved interfaces in thermodynamic equilibrium. This pressure drop is called the Laplace pressure, Δp, given by the Young-Laplace equation as:

$$\Delta p = \gamma \left(\frac{1}{R_1} + \frac{1}{R_2}\right) \qquad (6)$$

where γ is the interfacial tension, and R_1 and R_2 are the principal radii of curvature.[18] To deform a droplet and change its radii of curvature requires pressure. The amount of pressure needed can be thought of as the difference between a droplet's deformed Laplace pressure and its initial Laplace pressure, or:

$$\Delta p_{def} = \Delta p_f - \Delta p_i \qquad (7)$$

$$\Delta p_{def} = \gamma \left[\left(\frac{1}{R_{1f}} + \frac{1}{R_{2f}}\right) - \left(\frac{1}{R_{1i}} + \frac{1}{R_{2i}}\right)\right] \qquad (8)$$

Because the constriction only changes one principal radius, we can assume that R_{2F} and R_{2I} are equal, yielding:

$$\Delta p_{def} = \gamma \left(\frac{1}{R_{1f}} - \frac{1}{R_{1i}}\right) \qquad (9)$$

To squeeze a droplet through a 20 micron constriction, it must decrease its radius of curvature from R_{1i} = 20 μm to R_{1f} = 10 μm. Plugging these values into Equation 9 gives a minimum required deformation pressure of 250 Pa.

To achieve flow in an array channel, the droplets must move in series. The total pressure needed at the entrance of the array channel can be estimated as the sum of the

pressure needed to deform each droplet, or $\Delta P_{tot} = 40 * \Delta p_{def} = 1$ x 10^4 Pa = 1.45 psi. Applying a pressure above this threshold will result in droplets flowing through the array channel at a velocity proportional to the applied pressure.

Experimental

Experimental results show good agreement with the theoretical pressure calculations to release droplets. When the pressure applied to the inlets was slowly increased, droplet release was first observed with a total pressure of 1.5 psi, with partial pressures of 0.6 psi applied to the bypass oil inlet and 0.45 psi applied to both the water and oil inlets. Figure 8 shows droplets squeezing between array chambers at this threshold pressure. The pressure was increased to the oil bypass channel first, and the pressure applied to the oil and water inlets was adjusted to prevent droplet back-flow from the reservoir to the inlets. This value is very close to the theoretical pressure calculated above, higher by only 0.05 psi. This discrepancy can be attributed to over-simplification of theoretical pressure calculations or a difference between the applied pressure and the actual pressure at the entrance of the array channels. Applying pressures greater than this resulted in droplets flowing through the array channel at a velocity proportional to the applied pressure.

The effects of compliance were also observed during droplet generation and releasing. This phenomenon resulted in a delayed response between the droplets and the external pressure source. Thus, a 'loading' time was present when trying to release droplets and a 'cool-down' time was present which caused droplets to continue to release and flow when the external pressure was removed. The loading time decreased and the

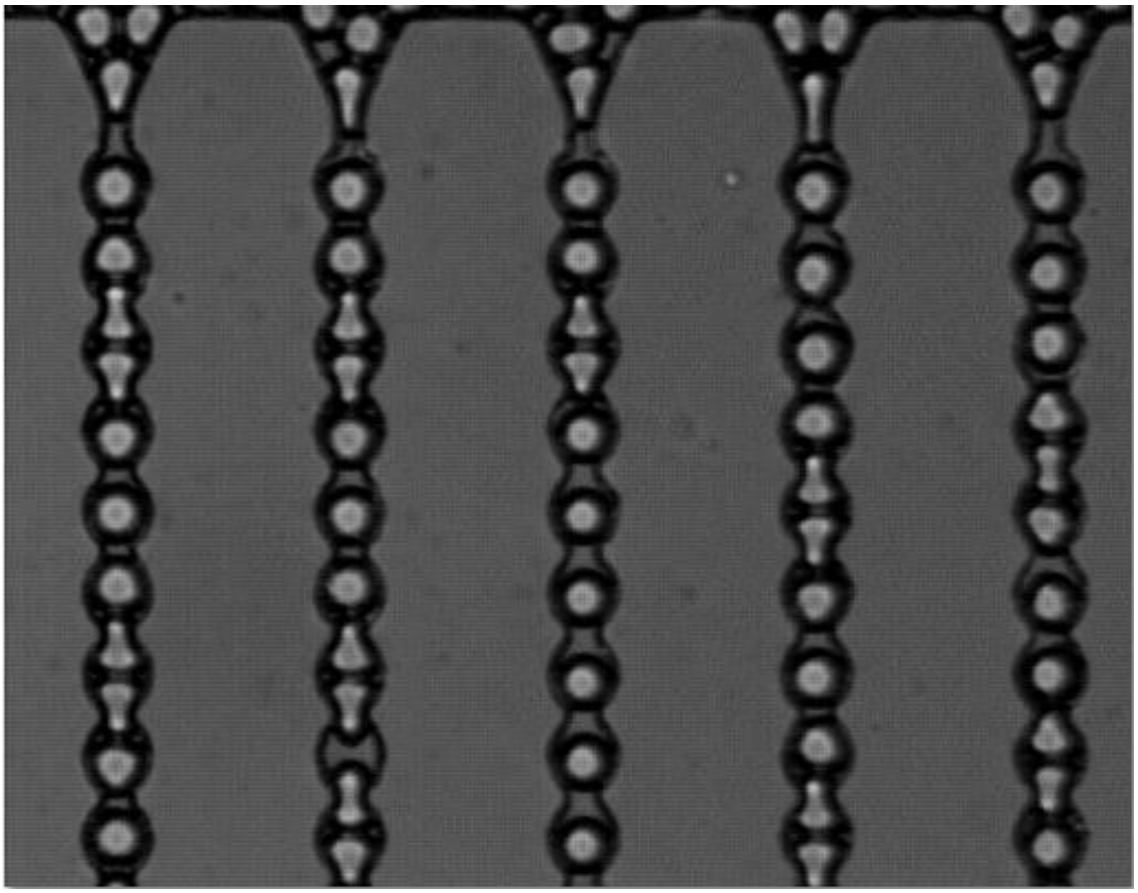

Figure 8: Photo of droplets squeezing through the constrictions between array chambers at total pressure of 1.5 psi.

cool-down time increased proportionally with pressure. The loading and cool-down times varied between 3-7 seconds with normal device operation. When conducting experiments with a device sealed with a PDMS coated glass slide, the response time was much shorter, less than 0.5 seconds. This illustrated the significance of membrane rigidity on response time. Another consequence caused by the elasticity of the thin film was droplet stacking within the reservoir, shown in Figure 9. While this effect cannot be completely avoided when operating a device sealed with a thin film membrane, it can be minimized by increasing the stiffness of the membrane and channels and operating the device at a lower pressure.

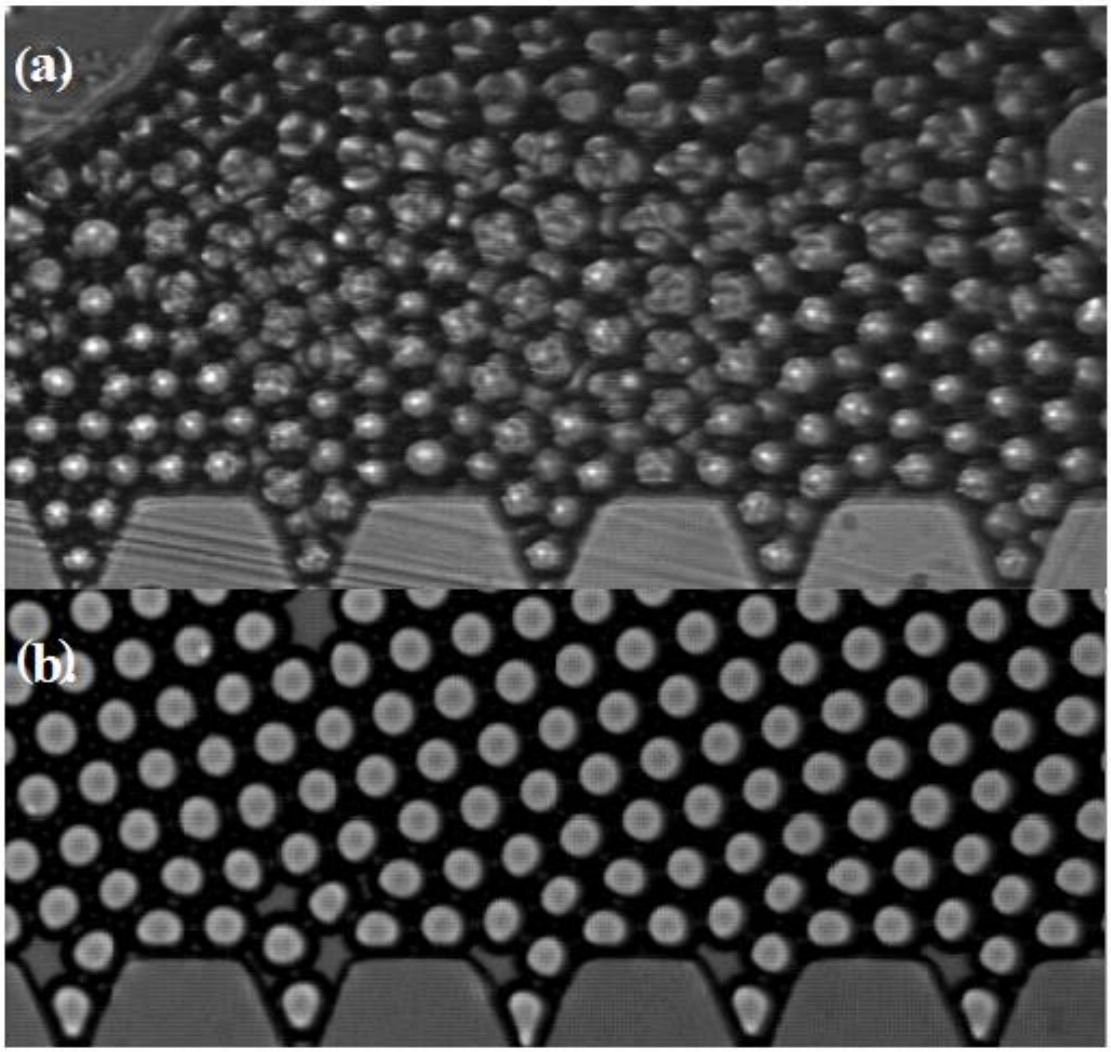

Figure 9: Elastic effects of the film observed by droplet stacking arrangements. (a) Device sealed with thin film demonstrations three dimensional stacking of droplets as the film expands. (b) Device sealed with a rigid PDMS-coated glass slide prohibits z-axis expansion and limits droplet stacking to a two dimensional arrangement.

Releasing droplets in each channel simultaneously proved to be impossible. However, various techniques were employed so that the overall release rate between the array channels was very similar. Array channels which have fewer droplets than other channels possess a lower hydraulic resistance and therefore released droplets at a higher rate. Small debris lodged in channels also impeded flow and lowered the release rate of

droplets within the obstructed channels. This indicates the importance of proper device cleaning and careful experimental set-up.

Droplet distribution and packing in front of the array channels (in droplet reservoir) also had a significant effect on the rates of droplet releasing between each channel. Array channels which had fewer droplets in front of its entrance released droplets at lower pressures and at a faster rate. This was again attributed to the difference in hydraulic resistance. This issue was often exacerbated with time, as the resistance in front of channels decreased with droplets releasing while other channels' resistances remained the same. A unique solution to combat this issue was discovered by applying a low pressure (<1.4 psi) for 10 minutes. This step caused the droplets to distribute more evenly across the channels and pack together closely. It is suspected that this occurred due to the motion of the continuous phase. The application of a low pressure caused the continuous phase to 'leak' through the array, but did not allow the droplets to release. The motion of the continuous phase dragged droplets with it towards the areas of least resistance. Eventually, equilibrium was achieved and the droplets distributed evenly across the entrance of the array channels in the reservoir.

Thin Film Design and Fabrication

Design Constraints and Optimization

Both the membrane and the device were constructed using a PDMS base to curing agent ratio of 5:1. A high curing agent ratio increases the stiffness of the channels and membrane. The relationship between Young's modulus and curing agent ratio is shown in

Figure 10.[24] This minimized the compliance of the device and the deflection of the membrane before puncture occurs. A large membrane deflection was undesirable because it can disrupt the contents of the microfluidic channel and push droplets into an adjacent array chamber. The membrane deflects similarly to Equation 3, except the pressure is replaced by a point force.

The maximum PDMS thin film thickness was limited by the length of the AFM probe tip. In order to give the probe access to the entire droplet, the combined height of the channel and thickness of the film cannot exceed the probe length. Because AFM probes are generally tapered, deeper probing will also enlarge the size of the access hole. Typically, probe tips are commercially manufactured between 10 to 15 microns in length. Longer tips up to 60 μm are also available. Therefore, if a channel height of 25 μm is specified, the

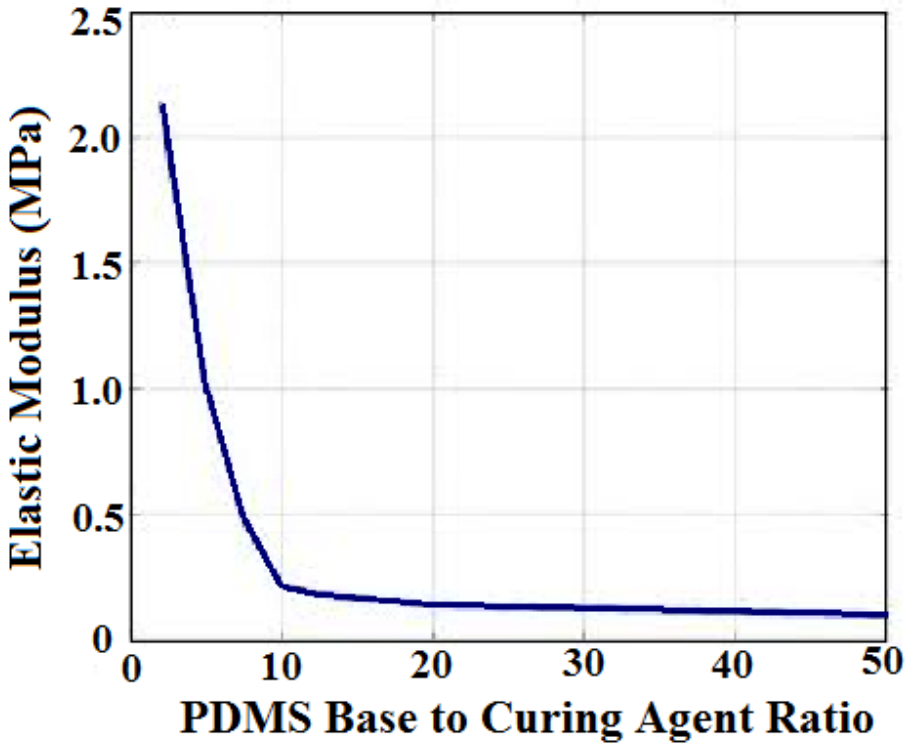

Figure 10: PDMS elastic modulus as a function of base to curing agent ratio[24]

maximum thickness of the thin film is 35μm before restricting the AFM probe's access to the bottom of the channel.

In addition, a thicker film requires more force to puncture through and will deflect more before being punctured. The increased force to puncture the film may affect the viability of aptamers hybridized onto the AFM tip for extraction. While the binding between streptavidin and biotin is one of the strongest, noncovalent biological interactions ($K_d = 10^{-14}$ M), the increased force needed to penetrate the thin film may result in damage to the surface of the aptamer.[23]

In this experiment, the PDMS thin film membrane was spun at 6000 rpm to yield an approximate thickness of 10 μm.

Fabrication

Two different methods were explored to fabricate the PDMS thin film and seal the device. After experimentation, one method was found to provide a simpler, faster fabrication process with a lower cost of materials.

The Solvent Release Method required the use of a resist and a solvent bath. Applying the resist onto the glass slide was time-consuming and tedious because it did not spread evenly over the slide and had to be applied over the entire slide. This also led to a lot of waste as the majority of the resist was spun off.

The release stage also presented some difficulties. First, extra care was required so the solvent did not enter the device through the inlets or outlets. Once solvent entered the device, the dissolved photoresist in the solvent would be trapped in the channels and harden as the acetone evaporated or diffused through the PDMS. Trying to remove this

solvent by pumping acetone and isopropyl alcohol through the device was an onerous process that did not work all the time. Using an adhesive tape proved ineffective because the adhesive was readily dissolved by a minute amount of acetone. Plugging the inlets and outlets with PDMS plugs also proved to be inadequate to blocking the solvent. And so, the most effective approach required the acetone level to be meticulously kept well below the surface of the device so that solvent could not enter the device.

Additionally, the porous nature of PDMS caused it to swell as it absorbed acetone. Because the acetone only contacted the bottom half of the device in the shallow bath, the bottom half expanded while the top half remained the same. This led to device warping. Warping often forced the thin film over the droplet reservoir area to contact the bottom of the channel and stick. Once stuck together, it was found to be impossible to separate the two layers without breaking the thin film. To attempt to combat the warping, a glass slide was bonded to the top of the device, providing a scaffold to keep the device flat. However, it was discovered that the lack of warping actually prevented the solvent from effectively reaching the resist, even when a mechanical wedge was used and acetone was injected between the device and glass slide. Using a more flexible scaffold such as a thin plastic in place of the glass slide yielded similar results.

Because of these issues, the Peel Method was much more attractive. The Mylar film is cheaper than the cost of materials needed in the Solvent Release Method, and the release step is shorter and less complex. The Peel Method did cause slight stretching of the PDMS film as it was peeled from the Mylar surface. Deformation was most apparent over the droplet reservoir area and when the Mylar film was peeled off quickly. Using a higher curing agent ratio helped combat this issue by stiffening the film. When peeling the Mylar

slowly from the device, the membrane did not deform significantly or droop to contact the substrate. Bending of the device was minimized by holding the microfluidic chip and peeling the Mylar of the chip, not vice versa. Bending the device after release did cause the thin film over the droplet reservoir to stick to the bottom of the substrate.

Although the benefits of the Peel Method over the Solvent Release Method were apparent in this research, I suspect there may be a limit to the minimum PDMS membrane thickness which can be fabricated via the Peel Method. As the thickness of the PDMS membrane decreases, the surface forces between the Mylar film and PDMS remain the same while the tensile strength of the membrane decreases. Tearing of the PDMS membrane may be inevitable below a certain thickness. The Solvent Release Method could produce ultra-thin PDMS films without mechanically straining the membrane.

Probing Simulation Validation

AFM probing was simulated by probing droplets using a mechanical micropositioner and a tungsten probe tip. The key differences between the AFM probe in Figure 1 and the tungsten probe (Figure 11) are listed in Table 1.[25] As seen in Table 1, the most significant differences between the AFM tip and the tungsten tip are the length, point diameter, and Young's Modulus. To understand if this simulation is valid, I evaluated how these differences would affect the probing process.

First, a larger point diameter requires a larger force to penetrate the film, resulting in a larger deflection of the film before it is punctured. The deflection of the PDMS film presses on the droplet, and if sufficient pressure is applied on the droplet by the film, droplets may be squeezed into an adjacent chamber. Unwanted droplet release is also

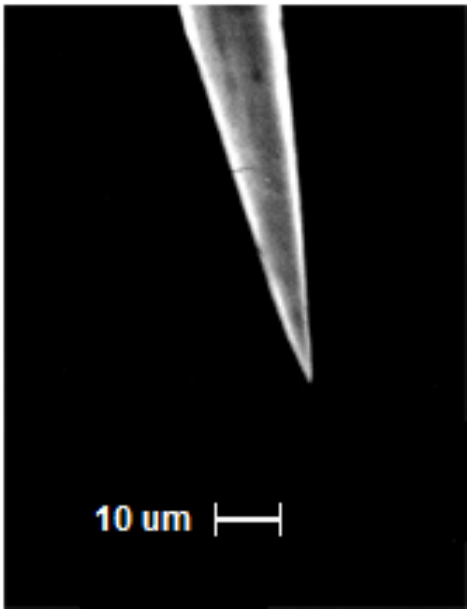

Figure 11: Scanning electron microscope image of a T-4-22 Tungsten probe point.[25]

influenced by the total volume of the tip entering the chamber. Therefore, unwanted droplet release will occur more readily with the larger and blunter tungsten tip than the AFM tip.

Next, the probe tip can fail via buckling if the compressive force experienced by the tip is great enough. The compressive strength of the tip before buckling can be determined by Euler's column formula:

$$F = \frac{n \cdot \pi^2 \cdot E \cdot I}{L^2} \qquad (10)$$

where n is the end condition factor, E is the elastic modulus, I is the area moment of inertia, and L is the length. The end conditions are shown in Figure 12.[26] The maximum allowable force before buckling is directly proportional to the elastic modulus and the area moment of inertia, and inversely proportional to the square of the length. The Young's moduli and the area moments of inertia are each within an order of magnitude with both

Table 1: Key differences between the AFM probe tip and the tungsten probe tip. Comparison of tips to validate probing simulation.

	AFM Probe Tip	Tungsten Probe Tip
Bulk Material	Silicon	Tungsten
External Material	Platinum	Tungsten
Shape	Concave Needle	Constant-Angle Needle
Length	15 – 30 μm	5100 μm
Point Diameter	0.1 – 0.4 μm	< 2.0 μm
Young's Modulus	150 GPa	400 GPa
Contact Angle with Water	40°	42°

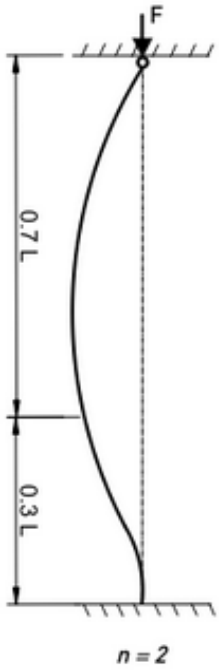

Figure 12: End conditions of probe tip puncturing thin film. One end is fixed and the other end is pinned (free to rotate).[26]

tips. Therefore, the maximum force before buckling is largely determined by the length squared. As the difference between the two tip lengths is over two orders of magnitude, it can be assumed that the AFM tip can withstand a much greater force before buckling,

indicating that failure via buckling should not occur with the AFM tip if the tungsten tip does not buckle.

Lastly, the surface interactions are considered. Both materials are fairly hydrophilic, with a contact angle of around 40° with water. The contact angle is given by Young's equation:

$$\gamma_{sv} - \gamma_{sl} = \gamma_{lv} \cdot \cos\theta \qquad (11)$$

where γ_{sv}, γ_{sl}, and γ_{lv} are the interfacial energies between the solid and vapor, solid and liquid, and liquid and vapor, respectively.[18] However, the tungsten probe has a larger surface area for the water droplet to wet. A larger surface area will result in a higher adhesion force between the tip and the water. Adhesion between the tip and water may result in the droplet splitting or the formation of small daughter droplets. Therefore, if droplets don't split while testing with the tungsten tip, droplet splitting should not occur with the smaller AFM tip.

After examining these considerations, we believe that despite the differences in size between the two tips, simulation of AFM probing is valid with the tungsten probe tip. Successfully probing the device with the tungsten tip indicates that the AFM tip will not buckle, cause droplets to release into an adjacent chamber, nor cause droplet splitting with similar operation.

Probing Simulation Results

The probing simulation yielded positive results. Puncturing the film did not cause droplets to be pushed into adjacent chambers, nor did it perturb droplets situated in adjacent chambers. Figure 13 shows the tungsten probe penetrating the thin film and

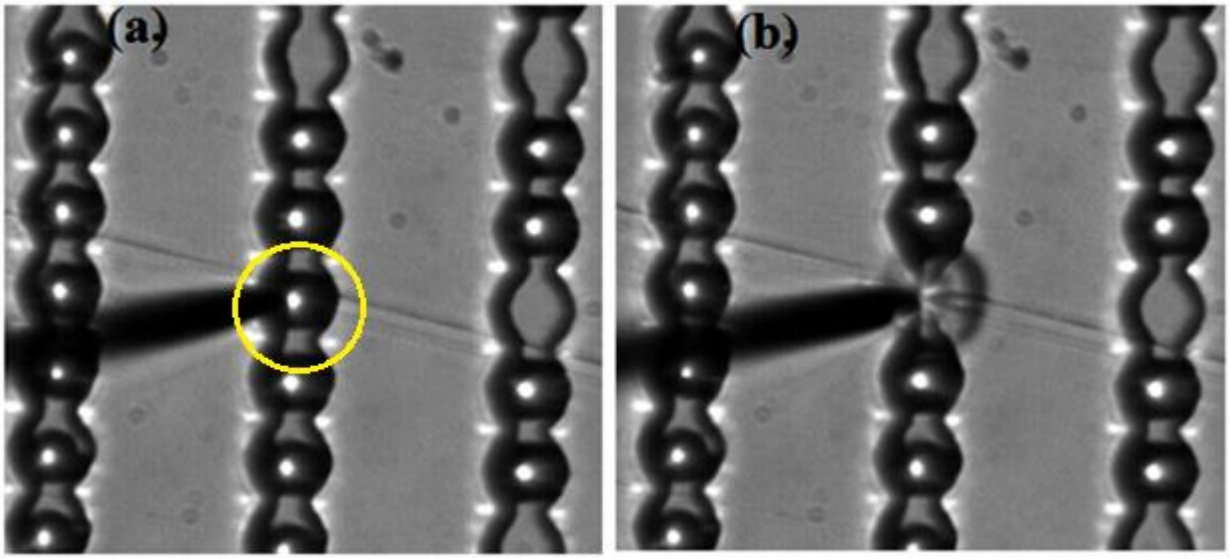

Figure 13: Photos of the tungsten probe accessing droplets (a) before puncturing the PDMS thin film (b) after penetrating thin film.

droplet. Deflection of the thin film while probing can be seen in Figure 13b. Because of the pointed shape of the tip, the thin film did not snap back once the needle penetrated the thin film. Instead, the local deflection was consistent as the probe penetrated the thin film. Deflection of the thin film was also observed with increased probe tip velocity. When the tip was retracted, the thin film deformed negatively due to the frictional force between the probe tip and the thin film. When puncturing the thin film with the blunt tungsten rod, the thin film deflected until snapping back slightly once the rod had penetrated through the thin film.

Additionally, probing droplets with the tungsten tip did not result in droplet splitting. Droplet splitting didn't occur even when the tip penetrated through the bottom of the channel, exposing the maximum amount of the probe's surface area to the water droplet. These results suggest that probing with the AFM tip will similarly not cause droplet splitting.

Droplet splitting was observed when probing the device with a tungsten rod with a 22 μm diameter. The rod was made by cutting off the sharp tip of the tungsten probe. Droplet splitting is shown in Figure 14. Droplet splitting was believed to be caused by either the increased membrane deflection caused by the blunt rod, the increased adhesion force resulting from the large surface area of the rod end, or a combination of the two. Volumetric displacement isn't believed to be a factor in this situation because neither event took place when the sharp probe tip passed through the bottom of the substrate.

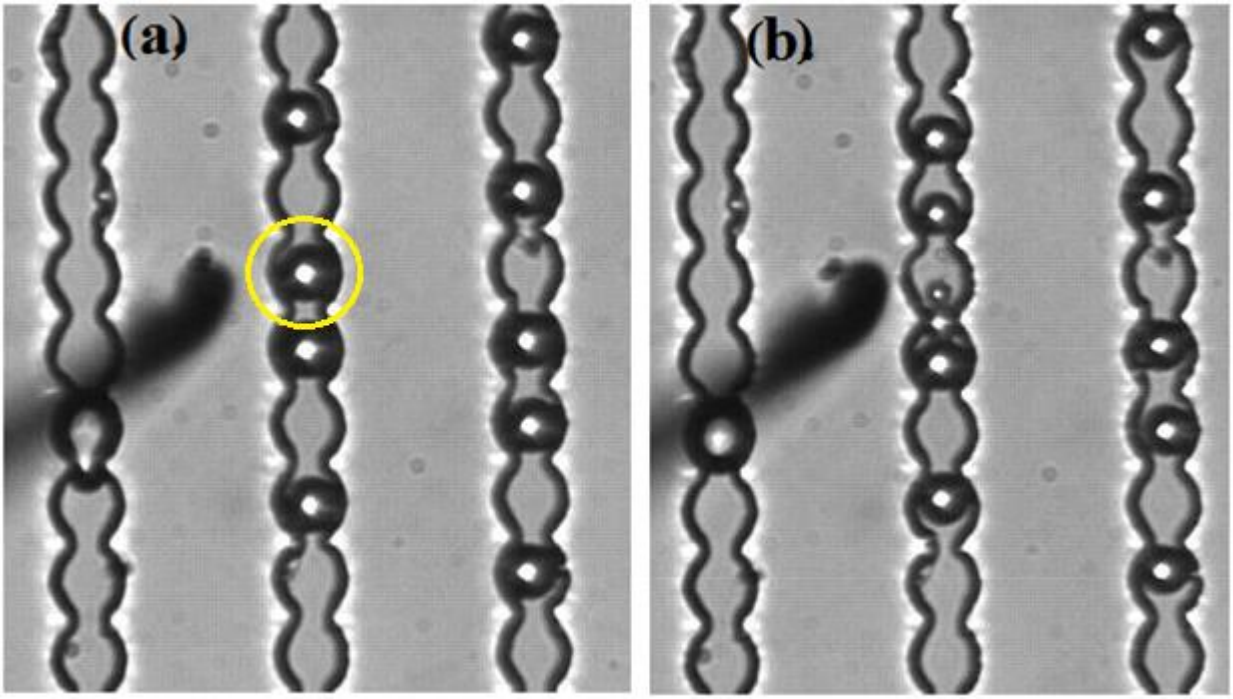

Figure 14: Photo of droplet splitting which occurred when puncturing the PDMS thin film to access droplets with a blunt tungsten rod (diameter of 22 microns).

CHAPTER 4: CONCLUSION

The atomic force microscope (AFM) has become an extremely powerful tool for biological and cell studies. However, the need for statistically significant sample sizes makes data collection an extremely lengthy process. In order to decrease data collection times, this research aimed to create a complementary microfluidic device to flow cells to the probe tip, immobilize cells while the probe investigates or manipulates the cell, and then release them to accept the next wave of cells.

This research has successfully demonstrated a microfluidic device sealed with a thin film membrane of PDMS which is capable of trapping and releasing droplets on demand. Sealing the device with a thin film membrane of PDMS provided access to physically probe the contents within the channels. The device also did not leak fluid, oil or water, through the access holes created mechanically with a 22 μm tungsten rod with an applied pressure of 4.5 psi. This held true even with over a dozen access points in the membrane.

The Peel Method was found to provide the simplest and most cost effective technique to fabricate and seal devices with a thin film of PDMS. Although there may be a minimum thickness limit for the Peel Method, it was not an issue in this research.

The next steps to continue this research would be to encapsulate live cells in aqueous droplets and conduct experiments with an AFM probe. Useful data to collect include maximum pressures before, oil leakage, droplet leakage, and membrane failure, with respect to membrane thickness. Other areas of interest to pursue include encapsulating cells with Dean flow to increase the single cell droplet efficiency.

REFERENCES

1. Joensson, Haakan N., and Helene Andersson Svahn. "Droplet Microfluidics-A Tool for Single-Cell Analysis." Angewandte Chemie International Edition 51, no. 49 (2012): 12176-2192.

2. Kemna, Evelien W. M., Rogier M. Schoeman, Floor Wolbers, Istvan Vermes, David A. Weitz, and Albert Van Den Berg. "High-yield Cell Ordering and Deterministic Cell-in-droplet Encapsulation Using Dean Flow in a Curved Microchannel." Lab on a Chip 12, no. 16 (2012): 2881-7.

3. Köster, Sarah, Francesco E. Angilè, Honey Duan, Jeremy J. Agresti, Anton Wintner, Christian Schmitz, and David A. Weitz. "Drop-based Microfluidic Devices for Encapsulation of Single Cells." Lab on a Chip 8, no. 7 (2008): 1110-5.

4. Holt, Daniel J., Richard J. Payne, Wing Ying Chow, and Chris Abell. "Fluorosurfactants for Microdroplets: Interfacial Tension Analysis." Journal of Colloid and Interface Science 350, no. 1 (2010): 205-11.

5. Baret, Jean-Christophe. "Surfactants in Droplet-based Microfluidics." Lab on a Chip 12, no. 3 (2012): 422-33.

6. Shibata, Takayuki, Kenji Nakamura, Shuhei Horiike, Moeto Nagai, Takahiro Kawashima, Takashi Mineta, and Eiji Makino. "Fabrication and Characterization of Bioprobe Integrated with a Hollow Nanoneedle for Novel AFM Applications in Cellular Function Analysis." Microelectronic Engineering 111 (2013): 325-31.

7. Bogle, Brittany, Horacio Espinosa, and Owen Loh. "Nanofountain Probes for Single-Cell Transfection: A Comparative Study Assessing Invasiveness." Nanoscape 7, no. 1 (2010): 33-37.

8. Nawarathna, D., T. Turan, and H. K. Wickramasinghe. "Selective Probing of MRNA Expression Levels within a Living Cell." Applied Physics Letters 95, no. 8 (2009): 083117.

9. Nawarathna, D., and H. K. Wickramasinghe. “United States Patent: US 8,365,311 – Selective Probing of MRNA Expression Levels within a Living Cell”, January 29, 2013.

10. Heinzelmann, Harry, Andre Meister, Philippe Niedermann, Michael Gabi, and Pascal Behr. "NADIS: A Novel AFM-based Tool for Dispensing Fluids into Single Cells." Microscopy and Analysis 23, no. 6 (2009): 11-13.

11. Meister, André, Michael Gabi, Pascal Behr, Philipp Studer, János Vörös, Philippe Niedermann, Joanna Bitterli. "FluidFM: Combining Atomic Force Microscopy and Nanofluidics in a Universal Liquid Delivery System for Single Cell Applications and Beyond." Nano Letters 9, no. 6 (2009): 2501-507.

12. Guillaume-Gentil, Orane, Eva Potthoff, Dario Ossola, Clemens Franz, Tomaso Zambelli, and Julia Vorholt. "Force-controlled Manipulation of Single Cells: From AFM to FluidFM." Trends in Biotechnology 32, no. 7 (2014): 381-88.

13. Favre, Mélanie, Jérôme Polesel-Maris, Thomas Overstolz, Philippe Niedermann. "Parallel AFM Imaging and Force Spectroscopy Using Two-dimensional Probe Arrays for Applications in Cell Biology." Journal of Molecular Recognition 24, no. 3 (2011): 446-52.

14. Oliveira, Nuno M., Ana I. Neto, Wenlong Song, and João F. Mano. "Two-Dimensional Open Microfluidic Devices by Tuning the Wettability on Patterned Superhydrophobic Polymeric Surface." Applied Physics Express 3, no. 8 (2010): 085205.

15. Jowhar, Dawit, Gus Wright, Philip C. Samson, John P. Wikswo, and Christopher Janetopoulos. "Open Access Microfluidic Device for the Study of Cell Migration during Chemotaxis." Integrative Biology 2, no. 11-12 (2010): 648-58.

16. Ballerini, David R., Xu Li, and Wei Shen. "Patterned Paper and Alternative Materials as Substrates for Low-cost Microfluidic Diagnostics." Microfluidics and Nanofluidics 13, no. 5 (2012): 769-87.

17. Huang, Shih-Hao, Wei-Heong Tan, Fan-Gang Tseng, and Shoji Takeuchi. "A Monolithically Three-dimensional Flow-focusing Device for Formation of Single/double Emulsions in Closed/open Microfluidic Systems." Journal of Micromechanics and Microengineering 16, no. 11 (2006): 2336-344.

18. Bruus, Henrik. Theoretical Microfluidics. Oxford [u.a.: Oxford Univ., 2010. Print.

19. Eaton, William, Fernando Bitsie, James Smith, David Plummer. “A New Analytical Solution for Diaphragm Deflection and its Application to a Surface Micromachined Pressure Sensor.” Paper presented at 2nd International Conference on Modeling and Simulation of Microsystems, San Juan, April 19-21, 1999.

20. Schmitz, Christian H. J., Amy C. Rowat, Sarah Köster, and David A. Weitz. "Dropspots: A Picoliter Array in a Microfluidic Device." Lab on a Chip 9, no. 1 (2009): 44-49.

21. MicroChem SU-8 2000 Permanent Epoxy Negative Photoresist. “PROCESSING GUIDELINES FOR: SU-8 2025, SU-8 2035, SU-8 2050 and SU-8 2075SU”.

22. Samuel, R., H J Sant, F. Jiao, C R Johnson, and B K Gale. "Microfluidic Laminate-based Phantom for Diffusion Tensor-magnetic Resonance Imaging." Journal of Micromechanics and Microengineering 21, no. 9 (2011): 950271-502711.

23. Wong, Joyce, Ashutosh Chilkoti, and Vincent T Moy. "Direct Force Measurements of the Streptavidin–biotin Interaction." Biomolecular Engineering 16, no. 1-4 (1999): 45-55.

24. Liu, Miao, and Quanfang Chen. "Characterization Study of Bonded and Unbonded Polydimethylsiloxane Aimed for Bio-micro-electromechanical Systems-related Applications." Journal of Micro/Nanolithography, MEMS and MOEMS 6, no. 2 (2007): 023008.

25. "Tungsten Probe Tips T-4 Series." Picoprobe Model T-4 Series Tungsten Probe Tips. Accessed August 9, 2014. http://www.ggb.com/t-4.html.

26. "Euler's Column Formula." Euler's Column Formula. Accessed November 26, 2014. http://www.engineeringtoolbox.com/euler-column-formula-d_1813.html.